Saudi Pharmaceutical Journal 32 (2024) 102045

HOSTED BY

Contents lists available at ScienceDirect

Saudi Pharmaceutical Journal

journal homepage: www.sciencedirect.com

The effect mechanism of ergosterol from the nutritional mushroom *Leucocalocybe mongolica* in breast cancer cells: Protein expression modulation and metabolomic profiling using UHPLC-ESI-Q

Asmaa Hussein Zaki [a,b,c], Bao Haiying [a,b,*], Mohamed Mohany [d], Salim S. Al-Rejaie [d], Bahaa Abugammie [e]

[a] Key Laboratory of Edible Fungi Resources and Utilization, Ministry of Agriculture and Rural Affairs, Jilin Agricultural University, Changchun 130118, Jilin, China
[b] College of Chinese Medicine Materials, Jilin Agricultural University, Changchun 130118, Jilin, China
[c] Departments of Agricultural Chemistry, Faculty of Agriculture, Minia University, El-Minia 61519, Egypt
[d] Department of Pharmacology and Toxicology, College of Pharmacy, King Saud University, P.O. Box 55760, Riyadh 11451, Saudi Arabia
[e] Key Laboratory of Molecular Epigenetics of the Ministry of Education (MOE), Northeast Normal University, Changchun, China

ARTICLE INFO

Keywords:
Ergosterol
Breast cancer
Cell viability
Apoptosis
Protein expression

ABSTRACT

The ergosterol from mushrooms has gained significant ethnopharmacological importance in various cultures, including China, Japan, and Europe. This compound has been found to possess immune-boosting and anti-inflammatory properties, making it useful in the treatment of immune disorders. In this study, we focused on investigating the potential anticancer properties of ergosterol isolated from the edible mushroom *Leucocalocybe mongolica* in breast cancer cell lines. The ergosterol was purified and identified using advanced analytical techniques such as ESI-MS and NMR. We conducted cell proliferation assays on 4 T1 breast cancer cells to assess the cytotoxic effects of ergosterol. Furthermore, we analyzed the transcription levels of BAX, caspase-7, BCL-2, STAT-3, and PARP proteins using real-time PCR and Western blot analysis. Additionally, we employed non-targeted ultra-high-performance liquid chromatography and high-resolution mass spectrometry (UPLC-MS/MS) to study the potential mechanisms underlying the anticancer effects of ergosterol at the metabolomics level. The results demonstrated a significant reduction in cell viability and the induction of apoptosis upon treatment with ergosterol, especially at higher concentrations ($P < 0.05$). Moreover, ergosterol affected the expression of cancer-related genes, upregulating pro-apoptotic proteins such as BAX, caspase-7, and PARP, while down-regulating the anti-apoptotic proteins BCL-2 and STAT-3 ($P < 0.05$). Western blot analysis confirmed these findings and provided further evidence of ergosterol's role in inducing apoptosis. Metabolomics analysis revealed substantial changes in pathways related to amino acid, antioxidant, and carbohydrate metabolism. In conclusion, our study demonstrates that ergosterol exhibits anticancer effects by inducing apoptosis and modulating metabolic pathways in breast cancer cells.

1. Introduction

The mushroom *Leucocalocybe mongolica* has been utilized in traditional Chinese medicine for centuries to fortify the stomach and spleen, and also to bolster immunity. Within traditional Mongolian medicine, *L. mongolica* is incorporated into mutton soup as a tonic for lactating women, aiming to enhance their immunity and augment maternal milk secretion. *L. mongolica* comprises numerous bioactive components, including sterols, phenolic compounds, terpenoids, and polysaccharides (Wang et al., 2020). The utilization of natural compounds and from mushroom pharmaceuticals has a rich historical background within traditional medical systems, and its potential advantages in managing symptoms of cancer have garnered significant attention (Nandi et al., 2024). Also, Natural chemicals may improve conventional therapies while reducing side effects (Han et al., 1999)(Joseph et al., 2017). Among these, ergosterol is a prominent sterol found in edible mushrooms (Baker and Brown, 2019). Previous research reported that ergosterol has a pharmacological impact on oxidative stress (Yongxia

* Corresponding author at: Key Laboratory of Edible Fungi Resources and Utilization, Ministry of Agriculture and Rural Affairs, Jilin Agricultural University, Changchun 130118, Jilin, China (Bao Haiying).
E-mail address: baohaiying2008@126.com (B. Haiying).

https://doi.org/10.1016/j.jsps.2024.102045
Received 23 January 2024; Accepted 19 March 2024
Available online 23 March 2024

et al., 2020), immunological function, diabetes (Xiong et al., 2018), cancer (Chen et al., 2017), and other disorders (Rangsinth et al., 2023).

Breast cancer is among the second most prominent reasons for cancer deaths in women all over the world, below lung disease (Siegel et al., 2017). Astonishingly, in 2020, over two million women were get diagnosed with breast cancer. Approximately 800,000 of them died due to the disease (Sung et al., 2021). Moreover, the traditional treatment approaches for breast cancer typically include a combination of surgical interventions, chemotherapy, radiation therapy and targeted biological therapies. These modalities have significantly increased patient outcomes, lowered tumor burden, and eliminated disease recurrence. However, it is essential to recognize that these treatments often come with various side effects, which range from mild to severe, that can adversely affect patients' quality of life (Fisher et al., 2005). In recent years, there has been increasing attention to exploring alternative treatments for breast cancer, especially derivatives from natural sources.

In recent times, gene expression and metabolomics analysis has rapidly developed as a prominent discipline following proteomics, transcriptomics and genomics. It possesses numerous applications in several fields, such as drug development, microbial, plant and animal metabolism and disease diagnosis (Zhu et al., 2020) (Yan et al., 2020). Medical chemistry has employed metabolomics to evaluate prospective biomarkers and therapeutic targets for a lot of illnesses, such as breast cancer, colorectal cancer, hepatocarcinoma, lung cancer, and hepatocellular carcinoma (Zhao et al., 2014). To investigate the differential low-molecular-weight metabolites in the breast cancer cell lines before and after treatment with ergosterol, we evaluated gene expression by rt-PCR and western bolt. We employed a non-targeted ultra-performance liquid chromatography with a tandem mass spectrometry (UPLC-MS/MS) approach. The objective of our study is to explore the potential of ergosterol as an anti-breast cancer agent. We aim to investigate its anticancer activity and the underlying mechanisms of action in breast cancer cells through gene expression analysis using RT-PCR and Western blotting, as well as examining metabolic changes.

2. Materials and methods

2.1. Materials and reagents

The ergosterol has been purified from the edible mushroom L. mongolica and and identified by ESI-MS and NMR (Zaki and Bao, 2022). The chemicals reagents were used in LC-MS grade acetonitrile, formic acid, methanol and ammonium acetate were bought from CNW Technologies (Duesseldorf, Germany). Deionized-ddH_2O was obtained from the Millipore Milli-Q water purification system (Billerica, MA, USA). Acetic acid and methanol were obtained from Tedia Co. (Ohio, USA). Meanwhile, the Beyotime Institute of Biotechnology (Haimen, China) provided the cell counting kit-8 (CCK8) assay.

2.2. Cell culture

The 4 T1 breast cancer cells were obtained from Procell Life Science & Technology Co, Ltd, in Wuhan, China. The 4 T1 cells were kept in RPMI-1640 medium containing fetal bovine serum: antibiotics (streptomycin and penicillin)) 9:1:0.1). The cells were placed in a 5 % CO_2 humidified incubator (SHELLAB, USA) and maintained at a temperature of 37 °C.

2.3. Proliferation assay

The cytotoxicity of the cells was assessed using the CCK8. Breast cancer 4 T1 cells were placed onto a 96-well plate with a density of 5 × 10^5 cells per well and given a period of 24 h to adhere. After incubation, the cells were exposed to the purified compound dissolved in a mixture of 10 μL dimethyl sulfoxide (DMSO) and 1000 μL RPMI-1640 medium at (50, 100.00, and 200.00 μg/mL) concentrations for each ergosterol compound. Six replicates were performed for each concentration, and the cells were further incubated in a CO_2 incubator at 37 °C with 5 % CO_2 for 24 h. Following the incubation period, add 10 μL of CCK8 solution with a concentration of 5 mg/mL to each well, then incubate the cells for two extra hours at 37 °C with 5 % CO_2. Lastly, the absorbance of the drug-treated wells was measured by the ELISA reader Bio–Rad, Hercules, CA, USA) at 450 nm to determine the visual concentrations.

2.4. Quantitative real-time PCR analysis

An optimized rt-PCR system was established to measure the relative expression levels of BCL2 Associated X (BAX), B-cell lymphoma 2 BCL2 genes in the breast cancer 4 T1 cells. Total RNA extraction from approximately 30–100 μg of the target cell lines was performed using TRIzol extraction solution under the optimal conditions and protocol of the manufacturer (Invitrogen Co., United States). RNA concentration was determined by measuring A230 and A260 using a nanodrop, and RNA quality was evaluated through 1.8 % agarose gel electrophoresis. All RNA samples were promptly stored at −80 °C until further use. For cDNA synthesis, the RNA samples were reverse-transcribed using the TIANScript RT Kit (Tiangen Co., China) in triplicates, including a negative control RNA sample (without reverse transcriptase) to detect genomic DNA contamination. Primer pairs for the target genes in the rt-PCR system were selected based on the gene sequences available in the NCBI database and designed using Primer Premier 5 software (STable 14–16). The PCR program commenced with an initial denaturation step (95 °C /15 min.), followed by 40 cycles with a condition of 95 °C /10 sec., 58 °C /30 sec., and 72 °C / 30 sec. (denaturation, extension, and annealing, respectively). Agarose gel electrophoresis was employed for sample separation, and dissociation curves were analyzed to assess product quality. The expression levels of BCL-2 and BAX genes were calculated using the delta-delta Ct (ΔCt) equation (Rao et al., 2013), where ΔCt reflects the difference between the Ct value of the housekeeping gene and the target gene.

2.5. Western blotting

The quantitative and qualitative properties of BCL2 Associated X (BAX), B-cell lymphoma 2 BCL-2, Caspase-7, Poly [ADP-ribose] polymerase 1 (PARP) and Signal transducer and activator of transcription 3 (STAT3) proteins were analyzed using the western blot technique. The cell lines were incubated individually with the isolated compound ergosterol for 24 h. After incubation, the cells were centrifuged for 10 min at 10,000 rpm (discard the supernatant and store the pellet at −80 ℃ until further use). Protein isolation was performed following the method described by (Martins-Gomes and Silva, 2018). Three replicates were performed for each treated sample. About 20 mg of cells were combined with 200 to 400 μL of cell lysate solution containing 150 mM NaCl, 50 mM Tris Base, and 0.1 % SDS (pH 8.0). The lysed cells were centrifuged for 10 min at 10,625 xg (12,000 rpm), and the upper layers were collected. The Coomassie Brilliant Blue (CBB) method was used to determine the protein concentration, as reported by (Arndt et al., 2012). Total protein was resolved in a 15 % SDS polyacrylamide gel and then transferred to a PVDF fluorine membrane for overnight incubation at 4 °C with the primary antibodies against BCL2 Associated X BAX (1:1000), Bcl-2 (B-cell lymphoma 2) BCL-2 (1:1000), Caspase-7 (1:600), Poly [ADP-ribose] polymerase 1 PARP (1:200), Signal transducer and activator of transcription 3 STAT3 (1:800), and GAPDH (1:1000). Subsequently, After washing the membrane with TBST, it was exposed to a secondary antibody (purchased from Beijing Zhong Co., China) at a dilution of 1:3000. This incubation step took place at room temperature for 1 h. The specific bands on the membrane were identified by comparing their molecular weight to a marker, and the analysis was performed using Image J software.

2.6. Metabolomic analysis of exudate

2.6.1. Sample preparation cell

Six sets of replicates were created for the metabolomics study, consisting of both ergosterol-treated and control groups. For each replicate in the ergosterol-treated group, a culture dish containing 5×10^6 cells was treated with 200 μg/mL of ergosterol for a duration of 24 h. However, the control group's cells were treated with the same amount of DMSO. To ensure cell viability and prevent cytotoxicity, keep the final DMSO concentration in the ergosterol-treated and control groups below 0.1 % (Dietmair et al., 2010). Following the treatment, the cells were washed with 2 mL of ice-cold isotonic saline (0.9 % [w/v] NaCl) after the culture media was removed. This step was carried out to eliminate any remaining medium and halt cellular metabolism (Mamer et al., 2013). In order to extract the metabolites from the cell residue, 1 mL of pre-cooled methanol/acetonitrile/water (v/v, 2:2:1) was used and subjected to sonication for 1 h in ice baths and then incubated the mixture at −20 °C for 1 h. Subsequently, the mixture was centrifuged at 14,000 g and four °C for 20 min. The resulting supernatant was carefully transferred to a sampling vial for further analysis using LC-MS. To ensure the quality of the data for metabolic profiling, we created quality control (QC) samples by combining portions from all the samples, which represented the entire sample set. These QC samples were then used to normalize the data. The QC samples underwent the same preparation and analysis procedure in each batch as the experimental samples.

The dried extracts were subsequently dissolved in 50 % acetonitrile, and a disposable 0.22 μm cellulose acetate filter was used to filter each sample. The filtered samples were transferred into 2 mL HPLC vials and kept in −80 °C freezer until analysis.

2.6.2. UHPLC-MS/MS analysis

The metabolomics profiling experiment was conducted using state-of-the-art UPLC-ESI-QOrbitrap-MS equipment. The experimental configuration consisted of high-performance liquid chromatography (HPLC), a Shimadzu Nexera X2 LC-30AD instrument, paired with a Thermo Scientific Q-Exactive Plus mass spectrometer. The chromatographic separation was conducted using a 2.1 mm × 100 mm ACQUITY UPLC BEH Amide column with a particle size of 1.7 m (manufactured by Waters Inc., Ireland). The separation method used was hydrophilic interaction liquid chromatography (HILIC). Aqueous solutions containing 25 mM ammonium acetate and 25 mM ammonium hydroxide were used as the mobile phase, while 100 % acetonitrile was used as the stationary phase. The flow rate was maintained at 0.5 mL/min throughout the study. The chromatographic gradient started with a solution consisting of 95 % acetonitrile for a duration of 1 min, followed by a progressive reduction to 65 % over a period of 7 min. The initial value was afterward decreased to 35 % throughout a span of 2 min and sustained for a duration of 1 min. This was then promptly followed by a quick escalation to 95 % within a time frame of 0.5 min. Following the gradient, a re-equilibration time of two minutes was observed. Data collection was performed using both positive (POS) and negative (NEG) electrospray ionization (ESI) modes. The parameters for the hot electrospray ionization (HESI) source were set up as follows: The spray voltage was set at 3.8 kV in positive mode and 3.2 kV in negative mode. The temperature of the capillary was maintained at 320 °C. The flow rate of the sheath gas was recorded as 30 units, but the auxiliary gas flow rate was measured at 5 units. The temperature of the probe heater was adjusted to 350 °C, while the RF level of the S-lens was set to 50 °C.

The mass spectrometry (MS) data gathering was performed using an instrument that included a mass-to-charge ratio (m/z) range spanning from 80 to 1200 Da. The complete mass spectrometry scans were acquired at a high resolution of 70,000 at a mass-to-charge ratio (m/z) of 200. Furthermore, in the case of MS/MS scans, the resolution was established at 17,500 for a mass-to-charge ratio (m/z) of 200. The maximum injection time was modified to 100 ms (ms) for MS scans and 50 ms for MS/MS scans. During the process of MS/MS scans, a specific isolation window of 2 m/z was chosen to isolate precursor ions selectively. Additionally, the normalized collision energy for fragmentation was systematically adjusted at discrete levels of 27, 29, and 32. In short, this set of experiments used the Q-Exactive Plus mass spectrometer and ultra-performance liquid chromatography (UPLC) to study metabolomics. The use of the hydrophilic interaction liquid chromatography (HILIC) separation technique and the implementation of appropriate instrument parameters allowed the capture of extensive data in both positive and negative electrospray ionization (ESI) modes. This enabled a thorough examination of the metabolomic profile of the samples, yielding detailed insights.

2.6.3. Data pre-processing and filtering

The raw MS data underwent processing using MS-DIAL software, which handled peak alignment, retention time correction, and peak area extraction. Metabolite identification was performed based on MS/MS data (mass tolerance < 0.02 Da) and accurate mass (mass tolerance < 0.01 Da), which were compared to databases such as HMDB, MassBank, and other public repositories, as well as our own metabolite standard library. We preserved only those variables in the extracted-ion features that had more than 50 % non-zero measurement values in at least one group.

2.6.4. Multivariate statistical analysis

The raw data files from the UHPLC-MS/MS were analyzed via Thermo Fisher's Compounds Discoverer 3.1 (CD3.1) to perform peak alignment, peak selection, and quantification for each metabolite. Import the offline data (raw) file into the CD-search program (Thermo Scientific, USA, Compound Discoverer 3.1). The peaks of different samples are aligned based on the retention time deviation of 0.2 min and the mass variation of 5 ppm after checking parameters like retention time and mass-to-charge ratio. The peak areas are simultaneously quantified and the peaks are extracted based on the quality deviation of 5 ppm, signal-to-noise ratio of 3, signal strength deviation of 30 %, additive ion, minimum signal strength of 100000, and other information to improve identification accuracy. The calculated molecular formula was contrasted to the McCloud database. The data recognition and quantitative findings were achieved after using blank samples to eliminate background ions and QC samples to standardize the quantitative findings. The peaks were matched with the McCloud (https://www.mzcloud.org/), mzVault, and MassList databases to achieve accurate quantitative and relative quantitative results. The statistical software R (version 3.4.3), CentOS (version 6), and Python (version 2.7.6) were used to try standard transformations when the data were not normally distributed.

2.6.5. KEGG Enrichment analysis

We used the KEGG database (https://www.kegg.jp) and performed KEGG pathway analysis to determine the disturbed biological pathways. The KEGG enrichment analysis was performed on the differential metabolite data using Fisher's exact test, and multiple testing correction was implemented using the false discovery rate (FDR) method. At a nominal p-value threshold of 0.05, enriched KEGG pathways were considered statistically significant.

2.7. Statistical analysis

All data were provided as mean and standard deviation and analyzed with SPSS 20 software from Chicago, IL, USA. ANOVA was used to compare statistical differences between experimentally treated and untreated cells, followed by Duncan's post-hoc test. The graphs were created with the GraphPad Prism 8 software.

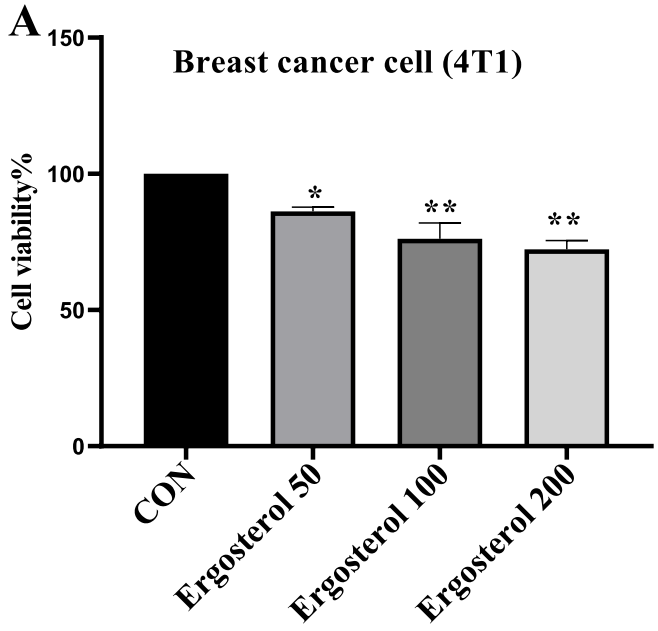

Fig. 1. The impact of ergosterol on the 4 T1 cell line's (A) 24-hour cell growth. The CCK8 assay was used to determine the viability of the cells, and the data are shown as the mean ± standard deviation (SD). Comparing the treatment group to the control group yielded statistically significant results (*P < 0.05, **P < 0.01), $n = 6$ in each group.

3. Results

3.1. Effects of ergosterol on cell viability

The impact of ergosterol on cell viability was assessed using the CCK8 assay. Breast cancer 4 T1 cells were treated with varying concentrations of ergosterol (50, 100, and 200 μg/ml) for a period of 24 h to investigate its effect on cell proliferation. The results revealed a significant increase in cytotoxicity in the treated cells, indicating that ergosterol treatment led to reduced cell viability ($P < 0.05$). At the concentration of 50 μg/ml, ergosterol induced apoptosis in 86.14 %, and at 100 μg/ml, ergosterol induced apoptosis in 76.11 % of the 4 T1 breast cancer cells. Furthermore, at the concentration of 200 μg/ml, the induction of apoptosis was 72.27 % ($P < 0.05$) (Fig. 1).

3.2. Ergosterol's effects on mRNA expression levels in breast cancer

Transcripted mRNA was evaluated in the cell lines by real-time PCR. BCL-2 and BAX transcription levels were assessed in 4 T1 cells treated with different concentrations of treated cells with ergosterol (50, 100 and 200 μg/ml). The mRNA expression of BAX was significantly increased in the ergosterol-treated 4 T1 cells when compared to the control group (Fig. 2) ($P < 0.05$,). Conversely, the mRNA expression of BCL-2 was found to be decreased in the treated 4 T1 cells with ergosterol (Fig. 2). These findings suggest that ergosterol may have an impact on the transcriptional regulation of BCL-2 and BAX in breast cancer cells ($P < 0.05$).

3.3. Impact of ergosterol on protein expression in breast cancer

Western blot analysis was employed to evaluate the protein expression levels of BAX, BCL-2, caspase-7, PARP, and STAT3. Treatment of breast cancer T41 cells with ergosterol resulted in a notable increase in BAX protein expression. In contrast, the expression of BCL-2 was observed to decrease in a concentration-dependent manner when compared to the control group ($P < 0.05$) (Fig. 3A, B). Consequently, the BAX/BCL-2 ratio was elevated, which regulates the balance between anti-apoptotic and pro-apoptotic factors implicated in mitochondrial function and apoptosis control. Inhibition of BCL-2 leads to activating the cytochrome *c*-mediated caspase pathway (Elmore, 2007). The PARP protein serves as a substrate for caspases and undergoes cleavage, leading to cell apoptosis. Ergosterol treatment dose-dependently increased the expression levels of caspase-7 and PARP proteins compared to the control group ($P < 0.05$) (Fig. 3C). The elevated expression of PARP supports the involvement of the caspase-mediated apoptosis pathway in 4TI cells (Fig. 3C, D). Furthermore, the JAK-STAT pathway plays a crucial role in the activation of various proteins associated with cancer apoptosis and metastasis. Also, the breast cancer cells treated with ergosterol exhibited a reduction in STAT-3 expression ($P < 0.05$) (Fig. 3E). In conclusion, these findings suggest that ergosterol significantly contributes to inducing apoptosis in breast cancer cells.

3.4. Assessment of the stability of metabolomics analysis methods

In this study, the researchers utilized the UHPLC-Q-Exactive LC-MS liquid mass spectrometry method to examine the overall changes in metabolites among different samples in groups. The quality control experiments demonstrated the stability of the instrumental analysis system, ensuring reliable and consistent experimental data. The observed differences in metabolic profiles accurately reflected the biological variations among the samples themselves. The experimental data was

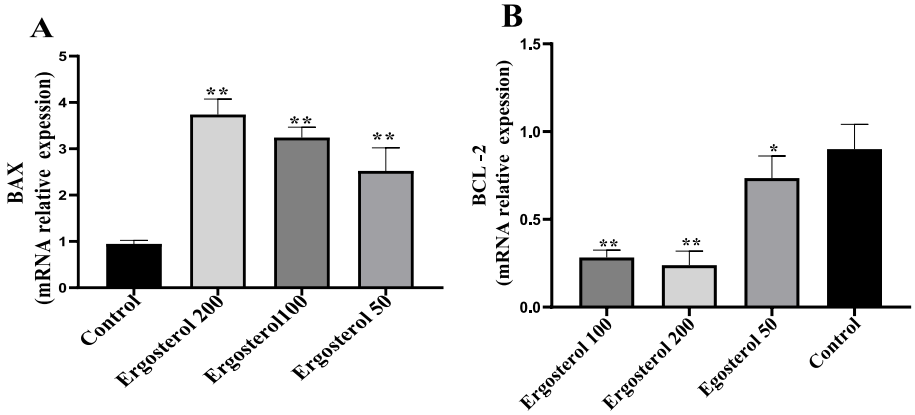

Fig. 2. Effect of ergosterol on the expression level of BAX (A), BCL-2 (B), caspase-7 (C), PARP (D) and STAT-3 in 4 T1 cells. The electrophoresis of the BAX, BCL-2, caspase-7, PARP and STAT-3 proteins. The typical images were detected by western blotting (F). Data are expressed as the mean values ± SD. Compared to untreated cells, *P < 0.05, **P < 0.01, $n = 10$ in each group.

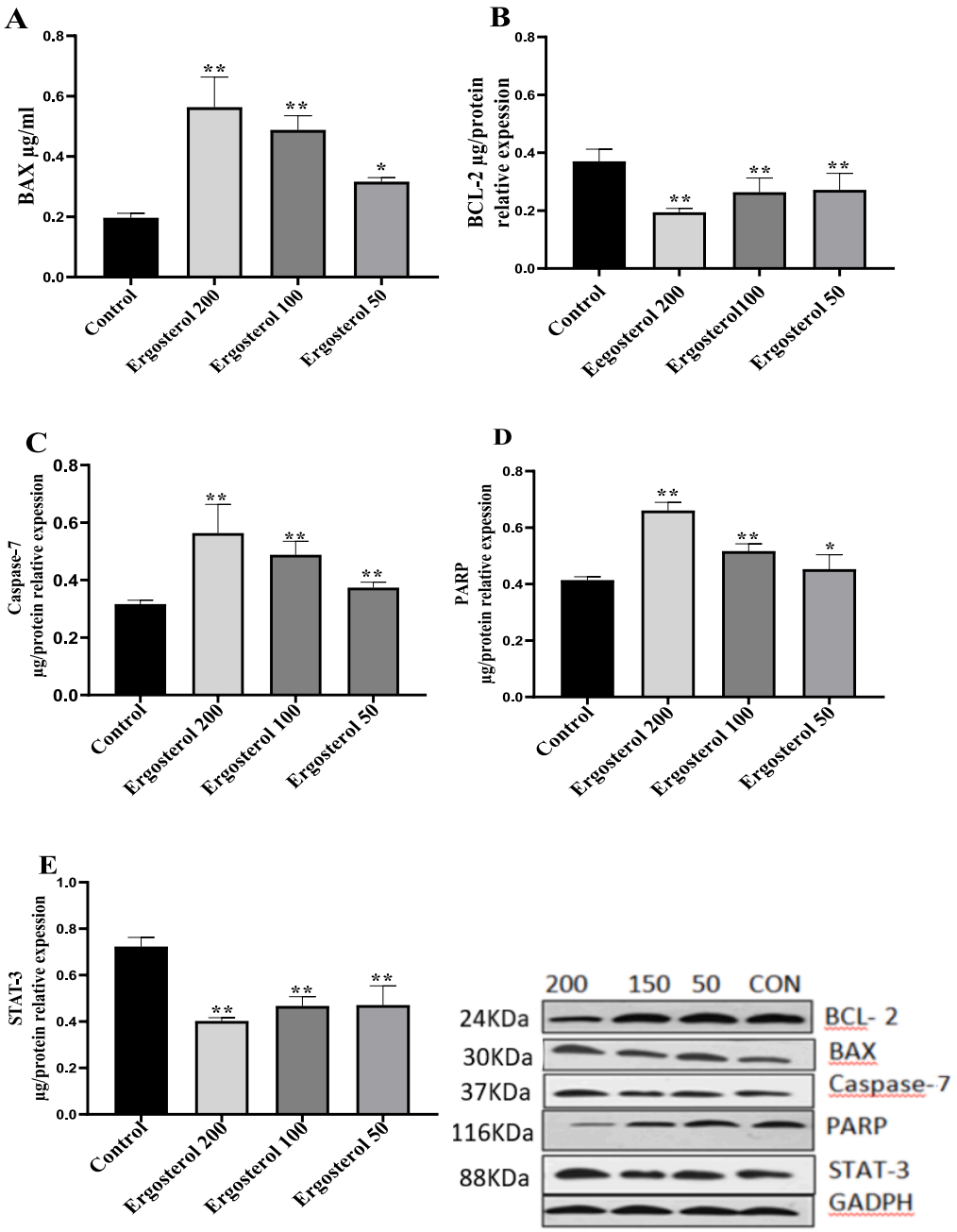

Fig. 3. Effect of Ergosterol on the Expression Levels of BAX (A), BCL-2 (B), Caspase-7 (C), PARP (D), and STAT-3 in 4 T1 Cells. Western blot analysis of BAX, BCL-2, Caspase-7, PARP, and STAT-3 proteins (E). Representative images detected by Western blotting are shown (F). Data are presented as mean values ± SD. *P < 0.05, **P < 0.01 compared to untreated cells, $n = 3$ in each group.

used to establish an OPLS-DA model, with R2 and Q2 values equal to or greater than 0.5, indicating the stability, reliability, and good explanatory and predictive abilities of the model Fig. 4. By employing the screening criteria of VIP (Variable Importance in Projection) > 1 and P-value < 0.05 within the OPLS-DA (Orthogonal Partial Least Squares Discriminant Analysis) model, several metabolites that showed significant differences were identified. These differentially expressed metabolites were further analyzed to investigate their expression changes and explore their involvement in functional pathways Fig. 4.

3.5. *Identification of ergosterol in metabolomic profiling of breast cancer*

To identify ergosterol among breast cancer metabolites, the researchers utilized the UHPLC-Q-Exactive LC-MS liquid mass spectrometry method to examine the overall changes in metabolites among different samples in groups. An untargeted metabolic assay was conducted on two sets of samples using U Q-Exactive Plus and PLC-Q-Exactive MS. The analysis successfully identified 359 positive (POS) metabolites and 293 negative (NEG) metabolites (Table S2). Multivariate data analysis techniques, including PCA (Principal Component Analysis) and OPLS-DA (Orthogonal Partial Least Squares Discriminant Analysis), were utilized to evaluate the variations of metabolites between breast cancer and ergosterol-treated samples. Fig. 5 a and b demonstrate the clustering of quality control samples, indicating good analytical stability and experimental reproducibility. The separation of two distinct sample groups is clearly observed based on the analysis of the first two principal components (PC1 and PC2), demonstrating notable distinctions in metabolite profiles between breast cancer cells

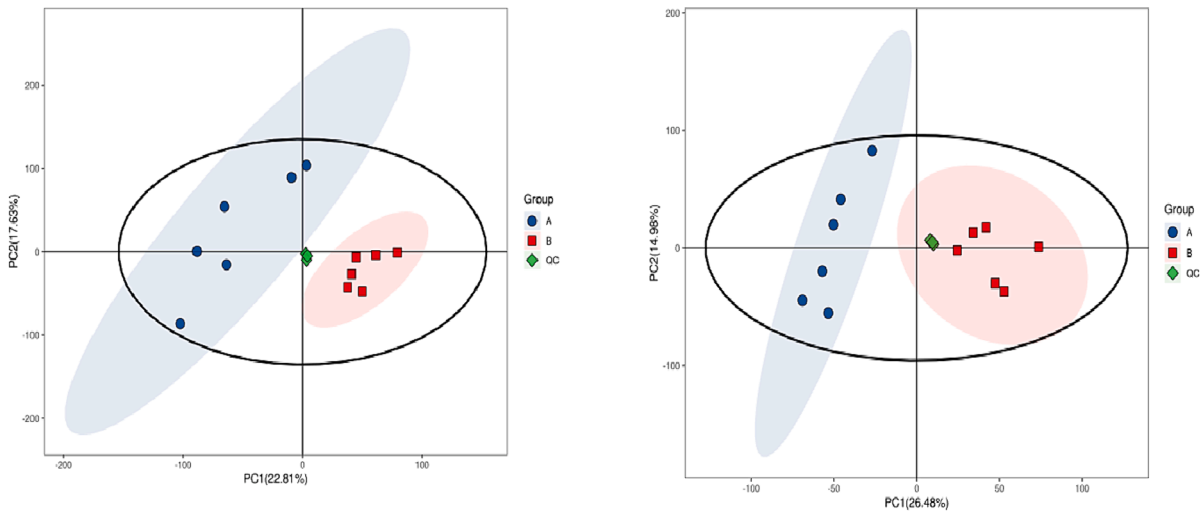

Fig. 4. Evaluation of Quality Assurance. (A–B) Quality assessment of positive and negative ion mode samples and quality control (QC) samples, $n = 6$ in each group.

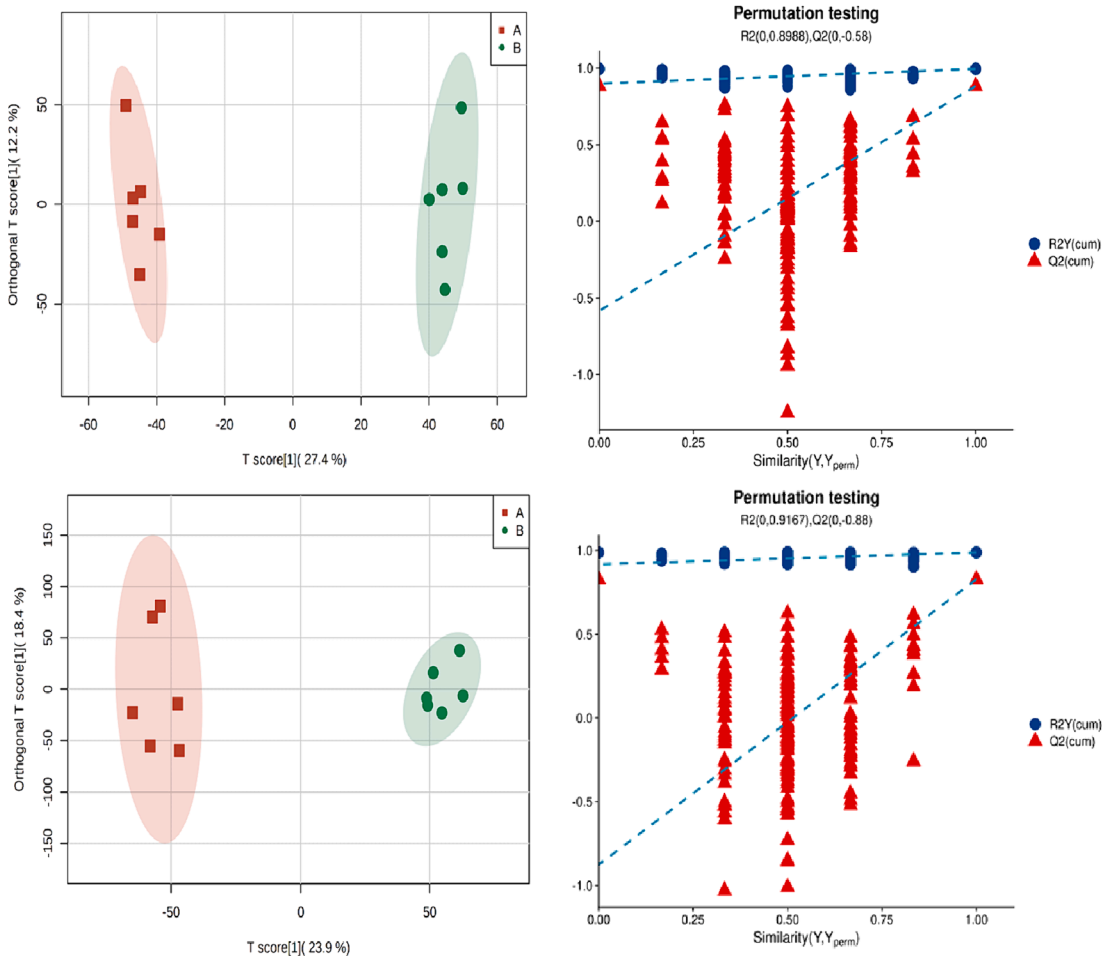

Fig. 5. Orthogonal Partial Least Squares Discriminant Analysis and principal component analysis. Plots showing samples' Principal Component Analysis scores that were obtained using POS. (b) Plots of samples' Principal Component Analysis scores that were obtained in NEG (c) Samples collected in POS with OPLS-DA score plots. (d) The OPLS-DA model's validation over 200 iterations of permutation testing in POS. (e) Properties of OPLS-DA score data for samples obtained in NEG. (f) 200 iterations of permutation testing in NEG to validate the OPLS-DA model. "QC" stands for quality control reference samples in the PCA analysis. The horizontal coordinates in the OPLS-DA represent the correlation between the original subgroup Y and the random subgroup Y. In contrast, the vertical coordinates represent the R2 and Q2 scores, where R2 represents the model's explanatory rate and Q2 represents its predictive power, $n = 6$ in each group.

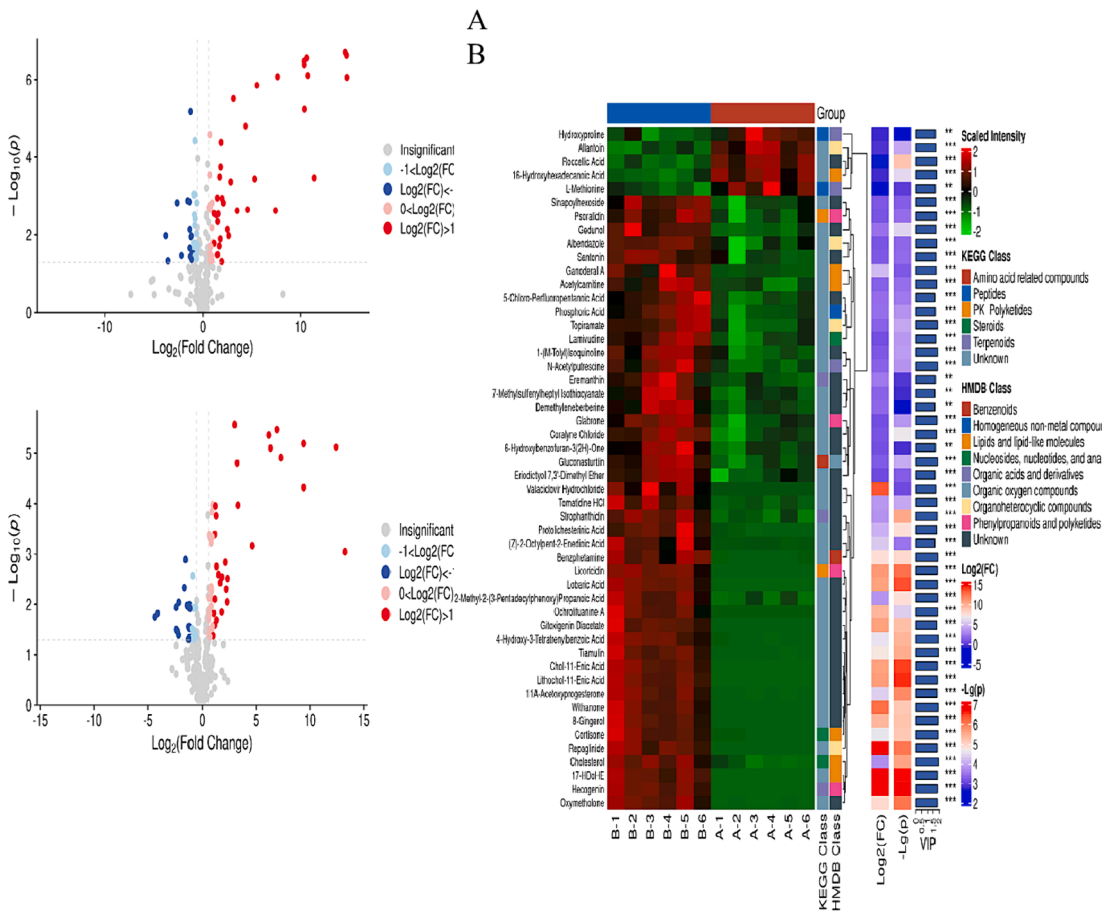

Fig. 6. Differential metabolite expression analysis between breast cancer cells treated with ergosterol and breast cancer cells. (A) the Volcano Plot illustrates the metabolic differences between breast cancer cells treated with ergosterol and breast cancer cells, red points indicate up-regulated metabolites, while blue dots represent down-regulated metabolites. (B) Hierarchical cluster analysis was employed to create a heat map showcasing the differential metabolites. The heat map includes the top 50 VIP (Variable Importance in Projection) values, $n = 6$ in each group.

and breast cancer mice treated with ergosterol.

To further improve the discrimination between breast cancer cell lines and ergosterol treatment in breast cancer, a supervised partial least squares discriminant analysis (PLS-DA) model was utilized. (Fig. S1). The partial least squares model exhibited high R2Y and Q2 values, indicating a strong fit and satisfactory predictive power. After excluding the quality control samples, the samples were subjected to Orthogonal Partial Least Squares Discriminant Analysis (OPLS-DA), a supervised statistical method for discriminant analysis. This method establishes a relationship model between metabolite expression and sample categories to predict sample classification. OPLS-DA is a modified version of Partial Least Squares Discriminant Analysis.

The figure below presents the model verification of OPLS-DA through 200 permutation tests. The x-axis represents the correlation between random group Y and original group Y, while the y-axis represents the R2 and Q2 scores. The quality of the multivariate statistical analysis model is determined based on the results of the permutation test. Suppose the Q2 regression line intercept is less than 0 or the Q2 score from the 200 permutation tests is lower than the Q2 score of the original model. In that case, it indicates the reliability of the model. The results suggest that the OPLS-DA model constructed based on the experimental data is reliable and effectively captures the changes in metabolites associated with breast cancer cells and ergosterol.

3.6. Hierarchical cluster analysis

The distinct metabolites between breast cancer cells treated with ergosterol and breast cancer cells are depicted in the volcano plot and clustering map (Fig. 6a and b). The analysis revealed that the expression of 140 metabolite species was upregulated, while the expression of 80 metabolite species was downregulated in the presence of ergosterol. In Fig. 6B, the top 50 differentially abundant metabolites are presented based on their abundance in breast cancer cells with ergosterol compared to breast cancer cells. The results highlight significant changes in the abundance of metabolic species in the breast cancer cell line following the administration of ergosterol. Such as the abundance of 1-(M−Tolyl)Isoquinoline, gedunol, cortisone, 8-gingerol, 2-methyl-2-(3-pentadecylphenoxy)propanoic acid, protolichesterinic acid, lobaric acid, glabrone increased significantly. Among the metabolites analyzed, hydroxyproline, L-methionine, 16-hydroxyhexadecanoic acid, roccellic acid, and allantoin exhibited significant decreases (Fig. 6a).

3.7. Metabolic pathway analysis

Metabolomic analysis tools, such as MetaboAnalyst and KEGG, were utilized to perform a topological analysis and identify potential biomarker enrichment in breast cancer with ergosterol. The figure presented below illustrates the results of this analysis. In the illustration, varying colors denote distinct first-level classifications, where more substantial areas signify a greater count of differential metabolites within each category. The accompanying legend offers details regarding the category's name, the quantity of differential metabolites, and the percentage they contribute to the pie chart.The major differential metabolites identified in breast cancer included peptides, alkaloids,

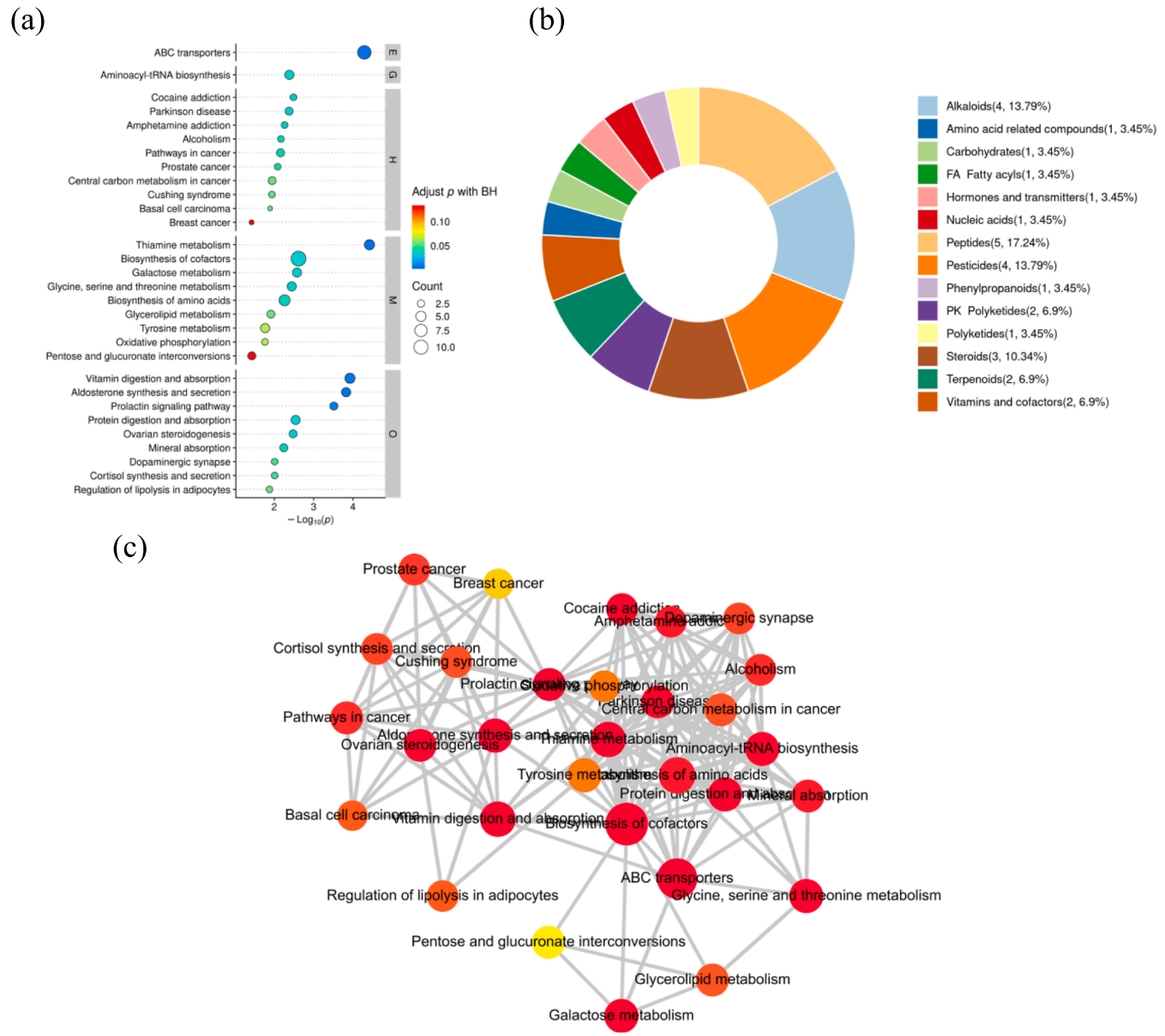

Fig. 7. (a) Classification of differentially metabolized pathways (KEGG) between breast cancer cells and breast cancer cells treated with ergosterol. (b) Bubble map depicting KEGG pathway enrichment in breast cancer cells and breast cancer cells with ergosterol treatment (top 30 pathways shown). Pathway classifications: M for metabolism, G for genetic information processing, C for cellular processes, E for environmental information processing, O for organismal systems, H for human diseases, D for drug development.. (c) Functional interaction networks of enriched pathways were mapped by identifying the 6 differentially expressed metabolites (DMs) associated with breast cancer cell line. Log10 (P) represents the log transformation applied to the ion abundance of metabolites identified by mass spectrometry. The "**" symbol indicates a P value of < 0.01 and the "*" symbol indicates a P value of < 0.05. Each dot on the graph represents a pathway, with the color indicating the P-value of the enrichment; the shade of red reflects the degree of enrichment. A larger circle indicates more annotated metabolites in that pathway (count). The presence of network lines connecting pathways signifies shared common DMs; the thickness of the line represents the number of metabolites shared between the pathways.

pesticides, steroids, terpenoids, vitamins and cofactors, PK polyketides, phenylpropanoids, and FA fatty acyls. The color of the circles in the figure represents the corresponding p-values, with darker colors indicating smaller p-values. The size of the circles represents the impact of the pathway, with larger circles indicating a greater impact. Additionally, KEGG pathway enrichment analysis was executed to explore the metabolic pathways linked to the differential metabolites subsequent to the intervention of ergosterol administration. The analysis identified several enriched pathways, including ABC transporters, aminoacyl-tRNA biosynthesis, protein digestion and absorption, tyrosine metabolism, thiamine metabolism, biosynthesis of cofactors, glycerolipid metabolism, prolactin signaling pathway, glycine, serine and threonine metabolism, galactose metabolism, oxidative phosphorylation, and biosynthesis of amino acids Fig. 7.

3.7.1. *Analysis of amino acid metabolic pathway*

In this study, we noted a noteworthy activation of several metabolic pathways, namely thiamine metabolism, and serine, glycine, tyrosine metabolism, and threonine metabolism, in breast cancer cells subsequent to treatment with ergosterol intervention. The levels of specific amino acids involved in these pathways, such as L-Threonine, L-Tyrosine, and 3,4-Dihydroxy-Phenylalanine, were notably elevated in breast cancer cells treated with ergosterol in comparison to untreated cells (Fig. 8 a b and c). These results imply that ergosterol could impact the

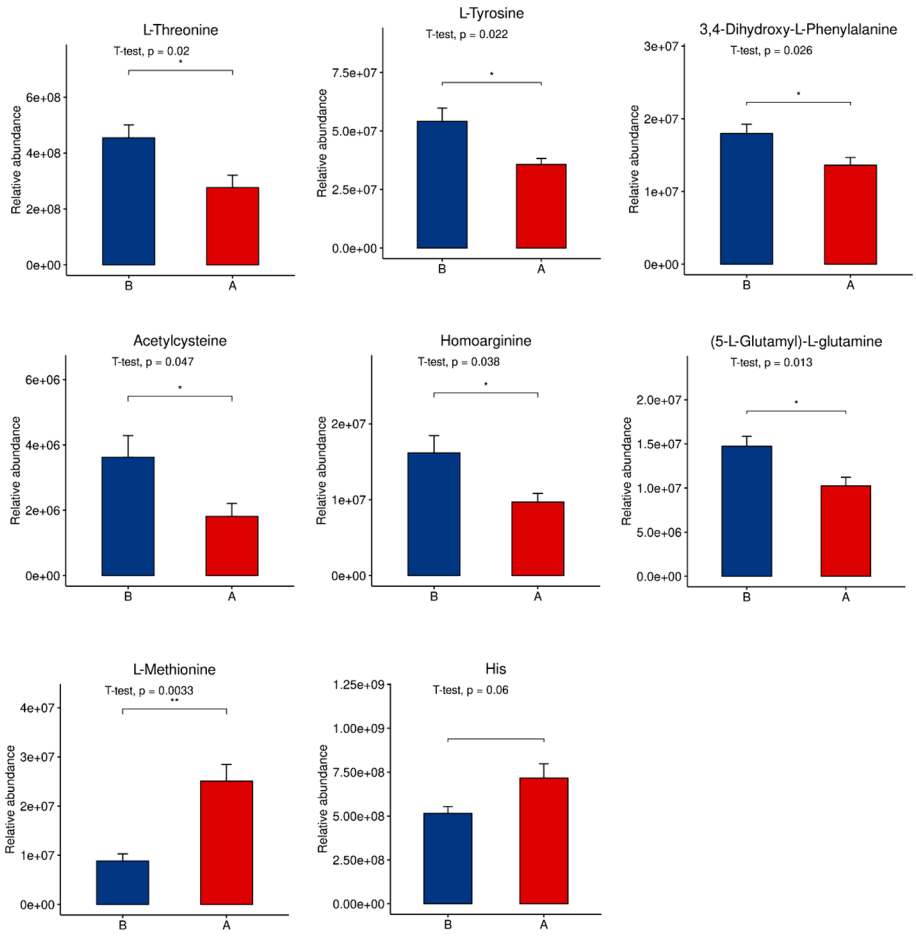

Fig. 8. Effect of Ergosterol Treatment on Amino Acid Levels.The figure illustrates the normalized intensity of specific amino acids, including L-Tyrosine, and 3,4-Dihydroxy-Phenylalanine homo-L-arginine, Acetylcysteine,(5-L-Glutamyl)-L-glutamine, methionine and histidine in different groups. The groups include the breast cancer cell line (A), and the ergosterol with breast cancer cell (B). The data are presented as (mean ± SD); each group consisted of 6 samples.

energy provision of branched-chain amino acids, modulate amino acid metabolism, and alleviate adverse nitrogen balance. Furthermore, the levels of homo-L-arginine, Acetylcysteine, and (5-L-Glutamyl)-L-glutamine, significantly increased in the ergosterol-treated breast cancer cells (Fig. 8). These changes indicate that ergosterol has the potential to enhance the immune system and inhibit tumor proliferation. While, methionine and histidine significantly decreased in the ergosterol-treated breast cancer cells (Fig. 8). Overall, our results suggest that ergosterol exerts its effects on breast cancer cells by modulating specific metabolic pathways, influencing amino acid metabolism, and potentially influencing immune function and tumor growth (see Figs. 8 and 9).

3.7.2. Metabolic pathway analysis of antioxidants

The levels of antioxidants were analyzed using LC-MS to assess their impact on breast cancer cells. After the intervention with ergosterol, the levels of flavonoids such as 5,7-dihydroxyflavanone, quercetin 3-O-malonylglucoside, theaflavin, and hecogenin were notably elevated in breast cancer cells compared to untreated cells (Fig. 10). Similarly, the levels of phenols, such as vanillin, were significantly elevated in breast cancer cells after ergosterol treatment. These findings suggest that ergosterol may contribute to increased antioxidant activity, potentially aiding in the inhibition and treatment of breast cancer (Fig. 10).

4. Discussion

Breast cancer is the most significant cause of cancer-related fatalities among women globally (Sung et al., 2021). While conventional anti-cancer chemical drugs can effectively target various types of cancer, they often come with potential short- or long-term side effects. Drug resistance further poses a significant challenge in cancer treatment, contributing to increased mortality rates (Tinoco et al., 2013). However, the development of multi-targeted approaches involving phytoconstituents and medicinal plants has shown promise. Our study is focused on exploring the impact of ergosterol obtained from the petroleum ether extract of *L. mongolica* on breast cancer, specifically the 4 T1 cell line. The results demonstrated that ergosterol effectively suppressed the growth of the 4 T1 breast cancer cell line. Notably, these findings are consistent with a study conducted by Wang et al. (2020), wherein significant dose-dependent growth inhibition was observed in HeLa, HepG2 and MCF–7 cells when treated with two ergosterols were isolated from the ethanol extract of *L. mongolica*, namely ergosta-4, 6, 8 (14), 22-tetraene-3-one (ET) and (22E, 24R)-ergosta-7, 22-diene-3β, 5α, 6β-triol (ED). In a previous investigation conducted by (Suriguge et al., 2012), it was discovered that the administration of petroleum ether extract (35 mg/kg) and ergosterol peroxide (5 mg/kg) obtained from *L. mongolica* fruit bodies effectively suppressed tumor growth in H22-bearing mice. The tumor rates were reduced by 69.61 % and 67.15 %, respectively. Moreover, both ergosterol and ergosterol peroxide demonstrated the ability to suppress the division of HepG2 cells and induce apoptosis, with apoptotic rates of 41.2 % and 42.33 %, respectively, during the early stages. These results suggest that the antitumor effects of ergosterols are mediated by the downregulation of VEGF and Bcl-2 expression upregulation of BAX protein expression and are dependent on the dosage of the compounds.

To explore the role of ergosterol in antiproliferation and apoptosis, we evaluated the expression levels of various anti-apoptotic and pro-

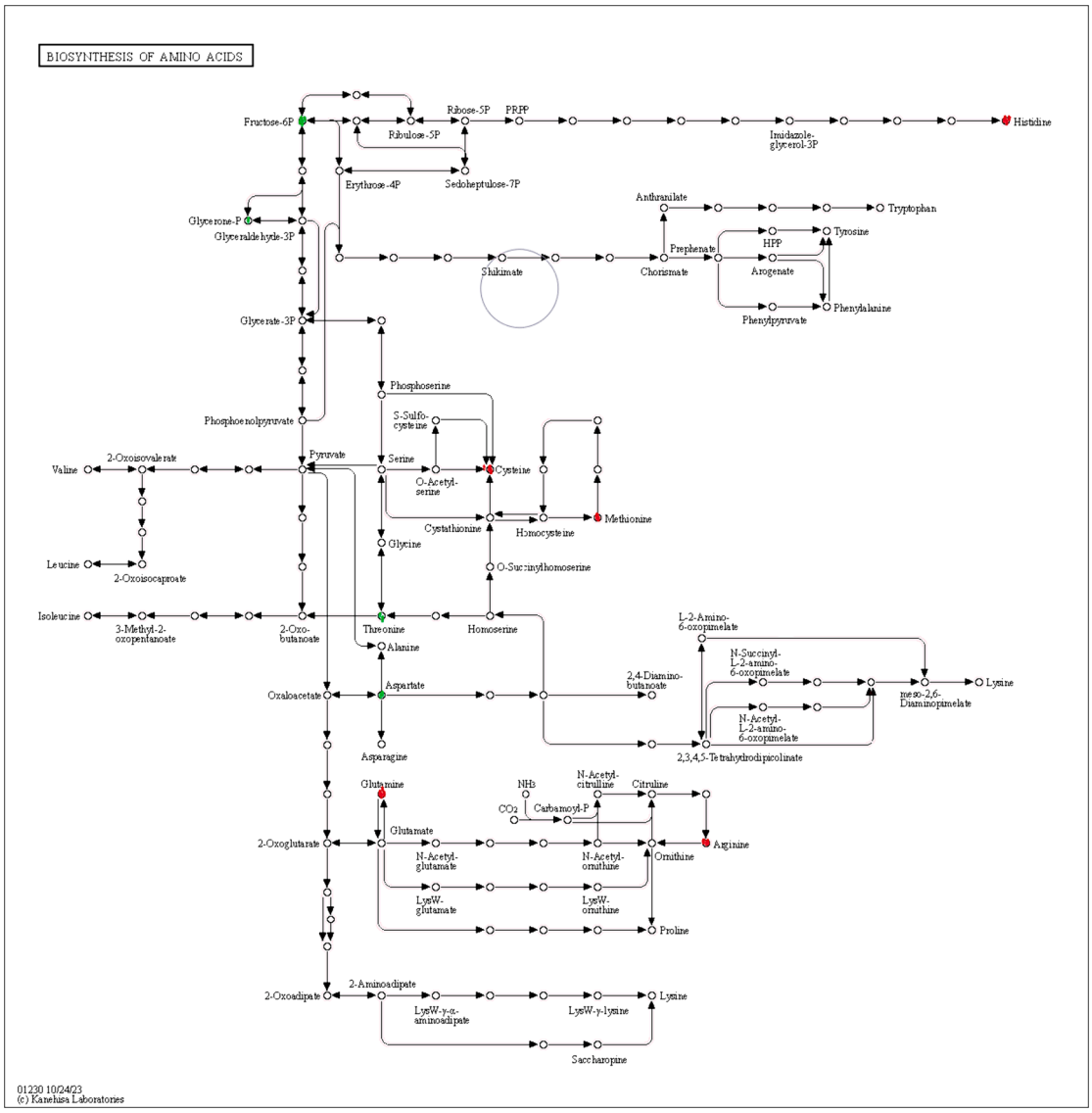

Fig. 9. KEGG enrichment pathway biosynthesis of amino acids. Green dot indicates up-regulated metabolite, red dot indicates down-regulated metabolite.

apoptotic proteins, such as BAX and BCL-2, in the treated cell lines. The BAX and BCL-2 family of proteins play a key role in regulating cell membrane permeability and the release of cytochrome *c* from mitochondria, which significantly influences the induction of apoptosis (Elmore, 2007). According to the results from western blot analysis, ergosterol led to an increase in the expression levels of BAX protein while simultaneously reducing the expression level of BCL-2 protein. This effect can be attributed to the stimulation of caspase overexpression through the release of cytochrome *c* from mitochondria, which contributes to the process. Similarly, a prior study found that two sterols from *L. mongolica* could elevate BAX protein levels and suppress BCL-2 in H22 tumor-bearing mice (Wang et al., 2020). The caspase family is involved in extrinsic pathways of apoptosis. Caspase-7 is a caspase family member that plays a vital role in programmed cell death(Elmore, 2007). The expression level of caspase-7 remarkably increased in the 4 T1 cells treated with ergosterol. During apoptosis, PARP protein acts as a substrate for caspases (Boulares et al., 1999); (Elmore, 2007) (Lazebnik et al., 1994). Therefore, the results indicated a substantial increase in the expression level of PARP and decreased STAT-3, which plays a pivotal role in governing diverse cellular processes, including cell proliferation and apoptosis (Yuan et al., 2004). Collectively, these findings corroborate the anticancer properties of ergosterol, as evidenced by its ability to enhance the expression of BAX, caspase, and PARP, while concurrently reducing BCL-2 and STAT-3 levels in the 4 T1 breast cancer cell line.

Interestingly, our study also revealed changes in metabolic analysis upon ergosterol treatment. The activation of pathways related to tyrosine metabolism, thiamine metabolism, and serine, glycine, and threonine metabolism in breast cancer cells indicates the involvement of ergosterol in amino acid metabolism. The higher levels of specific amino acids, such as L-Tyrosine and 3,4-Dihydroxy-Phenylalanine, in the ergosterol-treated breast cancer cells may influence cellular energy supply and contribute to the regulation of amino acid metabolism. Additionally, both tyrosine and phenylalanine are essential because they play a role as precursors in the production of catecholamines. They are a kind of neurotransmitters that act in a manner similar to that of adrenaline. It was previously shown that breast cancer cells have alterations in genes related to phenylalanine metabolism (Akkiprik et al., 2015). Some studies proposed that a high concentration and metabolites of phenylalanine cloud induce cell apoptosis(Zhang et al., 2007)(Ali et al., 2016). Additionally, the ergosterol-treated breast cancer cells increased significantly the levels of homo-L-arginine, Acetylcysteine, and (5-L-Glutamyl)-L-glutamine. Glutathione is abundantly distributed in different cell types which are composed of glutamate, cysteine, and glycine. It has a multifaceted function in carcinoma and antineoplastic

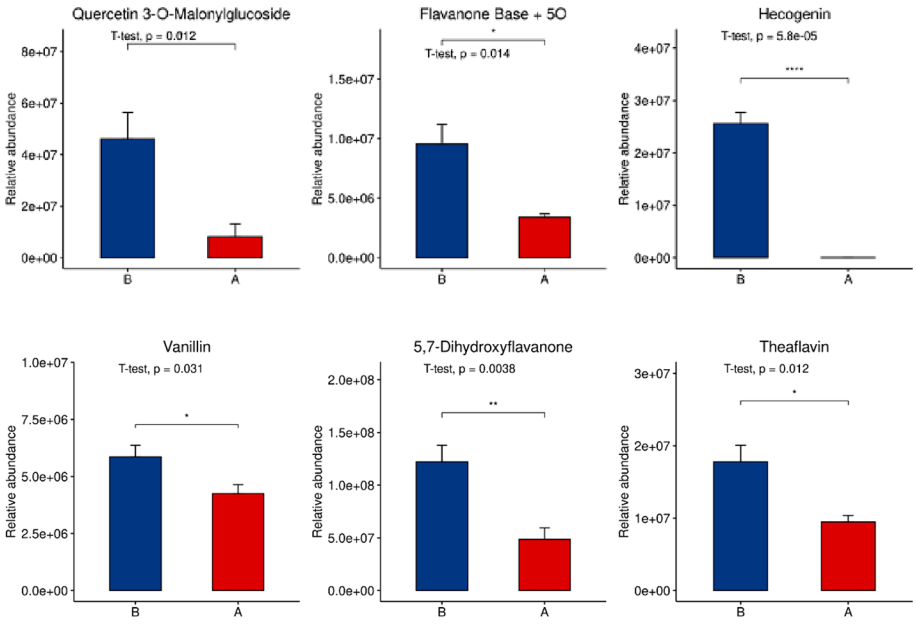

Fig. 10. Effect of Ergosterol Treatment on Metabolic pathway analysis of antioxidants. The figure illustrates the normalized intensity of specific amino acids, including 5,7-dihydroxy flavanone, quercetin 3-O-malonyl glucoside, theaflavin, and hecogenin, histidine and vanillin in different groups. The groups include the breast cancer cell line (A), and the ergosterol with breast cancer cell (B). The data are presented as the mean ± SD, and each group consisted of 6 samples.

treatment, including the removal of carcinogenic and the enhancement of immunity to chemotherapy for cancer (Balendiran et al., 2004).

Moreover, considering the well-known role of oxidative stress as a cause of cancer, the identification of antioxidants in breast cancer cells after treatment with ergosterol using LC-MS analysis further highlights the potential benefits of ergosterol in combating cancer and its association with oxidative stress modulation. Our results offered that ergosterol with breast cancer cell line leads to increased levels of phenols and flavonoids, indicating an enhanced antioxidant defense system.

Flavonoids have been commonly studied and recognized for their potential as anticancer agents (Zhao et al., 2019); Flavonoids have been seen to impede the growth of cancer cells by modulating the functions of reactive oxygen species (ROS)-scavenging enzymes. They also contribute to cell cycle arrest, induction of apoptosis and autophagy, and reduction in cancer cell proliferation and invasiveness (Kopustinskiene et al., 2020). A wide array of dietary phenolics has shown anticancer properties by exerting a multi-target impact on carcinoma of the breast cells and models of animals. These activities involve the control of cellular viability, growth, differentiation, and migration. Moreover, these chemicals exert regulatory effects on many signaling pathways, indicators associated with breast cancer, and the synthesis of proteins and genes (Losada-Echeberría et al., 2017)(Pan et al., 2015).

In this study, researchers utilized UHPLC-Q-Exactive LC-MS liquid mass spectrometry to investigate the impact of ergosterol from *L. mongolica* on breast cancer cells. Their analysis was thorough and included various statistical and analytical methods to ensure the stability and reliability of the results. They successfully identified differentially expressed metabolites using PCA, OPLS-DA, and PLS-DA techniques. The findings highlighted distinct metabolic profiles between breast cancer cells and those treated with ergosterol. Notably, the study demonstrated the potential of ergosterol to influence amino acid metabolism, antioxidants, and carbohydrate metabolism. Flavonoids and other metabolites were also identified as having elevated concentrations following ergosterol treatment. Importantly, these results were aligned with existing research on the anticancer effects of ergosterol and its impact on apoptosis-regulating proteins (Chen et al., 2017). This study provides valuable insights into the potential mechanisms underlying the anticancer activity of ergosterol and emphasizes the need for further investigation to comprehensively understand its implications.

In conclusion, this study employed a comprehensive approach to investigate the effects of ergosterol derived from *L. mongolica* on breast cancer cells. By utilizing advanced UHPLC-Q-Exactive LC-MS techniques and applying various analytical methods, the researchers were able to uncover significant metabolic changes induced by ergosterol treatment. The quality control experiments validated the stability of the analytical system, ensuring reliable and consistent data. The application of multivariate data analysis systems, including PLS-DA, OPLS-DA, and PCA, effectively highlighted the distinctions in metabolite profiles between breast cancer cells and those treated with ergosterol. These findings align with previous research (Rangsinth et al., 2023).

The study shed light on various metabolic pathways that were influenced by ergosterol, such as amino acid metabolism, antioxidants, and carbohydrate metabolism. The upregulation of specific metabolites, including flavonoids and amino acids, in response to ergosterol treatment, suggests its potential role in modulating key cellular processes. These findings align with previous research and provide deeper insights into the mechanisms behind the anticancer activity of ergosterol (Hao et al., 2017).

Furthermore, the study's rigorous approach to statistical validation and model testing enhances the reliability of the results. The correlation between experimental and biological variations underlines the accuracy of the observed metabolic differences. The confirmation of altered expression levels of key proteins, such as BAX, BCL-2, caspase3, and PARP, supports the notion that ergosterol exerts its effects by influencing apoptosis-related pathways. Ergosterol also diminishes positive angiogenesis regulators like VEGFC and STAT3 (Tan et al., 2017), broadening its potential as a breast cancer treatment by targeting both cancer cell survival and tumor vascularization.

In light of these findings, it is evident that ergosterol has the potential to be a valuable candidate in the development of novel therapeutic strategies for breast cancer. Nevertheless, further investigations are warranted to fully elucidate the exact mechanisms underlying the observed metabolic changes and their broader implications. Ultimately, this study contributes significantly to our understanding of the anticancer properties of ergosterol and highlights its promising role in the field of cancer research.

5. Conclusion

Ergosterol treatment showcased anticancer effects through the induction of apoptosis, substantiated by changes in gene and protein expression. Metabolomics analysis underscored noteworthy alterations in pivotal metabolic pathways. This research highlights the multifaceted mechanisms underpinning ergosterol's potential therapeutic impact on breast cancer cells. The findings accentuate the promising role of ergosterol in breast cancer research and therapy. This work needs additional *in vivo* experiments in animal models that could provide valuable insights into the efficacy and safety of ergosterol as a potential treatment for breast cancer. Animal studies allow us to evaluate the effect of compounds within a physiological context, including their bioavailability, distribution, metabolism, and potential toxicity.

Abbreviation

Leucocalocybe mongolica (L, mongolica), BCL2 Associated X (BAX), B-cell lymphoma 2 BCL-2, Caspase-7, Poly [ADP-ribose] polymerase 1 (PARP) and Signal transducer and activator of transcription 3 (STAT3) proteins, mass spectrometry (MS),ultra-performance liquid chromatography (UPLC) hydrophilic interaction liquid chromatography.

CRediT authorship contribution statement

Asmaa Hussein Zaki: Conceptualization, Writing – original draft, Formal analysis, Methodology. **Bao Haiying:** Conceptualization, Writing – review & editing, Supervision, Project administration, Software. **Mohamed Mohany:** Funding acquisition, Writing – review & editing, Supervision, Resources, Software. **Salim S. Al-Rejaie:** Writing – review & editing, Supervision, Resources. **Bahaa Abugammie:** Investigation, Formal analysis, Methodology, Resources.

Declaration of competing interest

The authors declare that they have no known competing financial interests or personal relationships that could have appeared to influence the work reported in this paper.

Acknowledgments

This work was supported by the National Natural Science Foundation of China (grant no. 31870014). The authors extend their appreciation to the Researchers Supporting Project number (RSPD2024R758), King Saud University, Riyadh, Saudi Arabia.

Appendix A. Supplementary data

Supplementary data to this article can be found online at https://doi.org/10.1016/j.jsps.2024.102045.

References

Akkiprik, M., Peker, İ., Özmen, T., Güllü Amuran, G., Güllüoğlu, B.M., Kaya, H., Özer, A., 2015. Identification of differentially expressed IGFBP5-related genes in breast cancer tumor tissues using cDNA microarray experiments. Genes (basel). 6, 1201–1214.

Ali, M.R.K., Wu, Y., Han, T., Zang, X., Xiao, H., Tang, Y., Wu, R., Fernández, F.M., El-Sayed, M.A., 2016. Simultaneous time-dependent surface-enhanced raman spectroscopy, metabolomics, and proteomics reveal cancer cell death mechanisms associated with gold nanorod photothermal therapy. J. Am. Chem. Soc. 138, 15434–15442.

Arndt, C., Koristka, S., Feldmann, A., Bartsch, H., Bachmann, M., 2012. Coomassie-brilliant blue staining of polyacrylamide gels. Methods Mol. Biol. 869, 465–469. https://doi.org/10.1007/978-1-61779-821-4_40.

Baker, M.A.B., Brown, A.J., 2019. A detour to sterol synthesis. Nat. Microbiol. 4, 214–215.

Balendiran, G.K., Dabur, R., Fraser, D., 2004. The role of glutathione in cancer. Cell Biochem. Funct. Cell. Biochem. Its Modul. by Act. Agents or Dis. 22, 343–352.

Boulares, A.H., Yakovlev, A.G., Ivanova, V., Stoica, B.A., Wang, G., Iyer, S., Smulson, M., 1999. Role of poly (ADP-ribose) polymerase (PARP) cleavage in apoptosis: caspase 3-resistant PARP mutant increases rates of apoptosis in transfected cells. J. Biol. Chem. 274, 22932–22940.

Chen, S., Yong, T., Zhang, Y., Su, J., Jiao, C., Xie, Y., 2017. Anti-tumor and anti-angiogenic ergosterols from ganoderma lucidum. Front. Chem. 5, 85.

Dietmair, S., Timmins, N.E., Gray, P.P., Nielsen, L.K., Krömer, J.O., 2010. Towards quantitative metabolomics of mammalian cells: development of a metabolite extraction protocol. Anal. Biochem. 404, 155–164.

Elmore, S., 2007. Apoptosis: a review of programmed cell death. Toxicol. Pathol. 35, 495–516.

Fisher, B., Costantino, J.P., Wickerham, D.L., Cecchini, R.S., Cronin, W.M., Robidoux, A., Bevers, T.B., Kavanah, M.T., Atkins, J.N., Margolese, R.G., 2005. Tamoxifen for the prevention of breast cancer: current status of the National Surgical Adjuvant Breast and bowel project P-1 study. J. Natl. Cancer Inst. 97, 1652–1662.

Han, S.B., Lee, C.W., Jeon, Y.J., Hong, N.D., Yoo, I.D., Yang, K.-H., Kim, H.M., 1999. The inhibitory effect of polysaccharides isolated from phellinus linteus on tumor growth and metastasis. Immunopharmacology 41, 157–164. https://doi.org/10.1016/S0162-3109(98)00063-0.

Hao, J., Zhang, X., Yu, W., Wang, R., Xue, Z., Kou, X., 2017. Identification and evaluation of bioactivity of compounds from the mushroom pleurotus nebrodensis (agaricomycetes) against breast cancer. Int. J. Med, Mushrooms, p. 19.

Joseph, T.P., Chanda, W., Padhiar, A.A., Batool, S., LiQun, S., Zhong, M., Huang, M., 2017. A preclinical evaluation of the antitumor activities of edible and medicinal mushrooms: a molecular insight. Integr. Cancer Ther. 17, 200–209. https://doi.org/10.1177/1534735417736861.

Kopustinskiene, D.M., Jakstas, V., Savickas, A., Bernatoniene, J., 2020. Flavonoids as anticancer agents. Nutrients 12, 457.

Lazebnik, Y.A., Kaufmann, S.H., Desnoyers, S., Poirier, G.G., Earnshaw, W.C., 1994. Cleavage of poly (ADP-ribose) polymerase by a proteinase with properties like ICE. Nature 371, 346–347.

Losada-Echeberría, M., Herranz-López, M., Micol, V., Barrajón-Catalán, E., 2017. Polyphenols as promising drugs against main breast cancer signatures. Antioxidants 6, 88.

Mamer, O., Gravel, S.-P., Choiniere, L., Chénard, V., St-Pierre, J., Avizonis, D., 2013. The complete targeted profile of the organic acid intermediates of the citric acid cycle using a single stable isotope dilution analysis, sodium borodeuteride reduction and selected ion monitoring GC/MS. Metabolomics 9, 1019–1030.

Martins-Gomes, C., Silva, A.M., 2018. Western blot methodologies for analysis of in vitro protein expression induced by teratogenic agents. Teratogenicity Testing. Springer 191–203.

Nandi, S., Sikder, R., Rapior, S., Arnould, S., Simal-Gandara, J., Acharya, K., 2024. A review for cancer treatment with mushroom metabolites through targeting mitochondrial signaling pathway: in vitro and in vivo evaluations, clinical studies and future prospects for mycomedicine. Fitoterapia 172, 105681. https://doi.org/10.1016/j.fitote.2023.105681.

Pan, M., Chiou, Y., Chen, L., Ho, C., 2015. Breast cancer chemoprevention by dietary natural phenolic compounds: specific epigenetic related molecular targets. Mol. Nutr. Food Res. 59, 21–35.

Rangsinth, P., Sharika, R., Pattarachotanant, N., Duangjan, C., Wongwan, C., Sillapachaiyaporn, C., Nilkhet, S., Wongsirojkul, N., Prasansuklab, A., Tencomnao, T., 2023. Potential beneficial effects and pharmacological properties of ergosterol, a common bioactive compound in edible mushrooms. Foods 12, 2529.

Rao, X., Huang, X., Zhou, Z., Lin, X., 2013. An improvement of the 2(-delta delta CT) method for quantitative real-time polymerase chain reaction data analysis. Biostat. Bioinforma. Biomath. 3, 71–85.

Siegel, R.L., Miller, K.D., Fedewa, S.A., Ahnen, D.J., Meester, R.G.S., Barzi, A., Jemal, A., 2017. Colorectal cancer statistics, 2017. CA. Cancer J. Clin. 67, 177–193.

Sung, H., Ferlay, J., Siegel, R.L., Laversanne, M., Soerjomataram, I., Jemal, A., Bray, F., 2021. Global cancer statistics 2020: GLOBOCAN estimates of incidence and mortality worldwide for 36 cancers in 185 countries. CA. Cancer J. Clin. 71, 209–249.

Suriguge, B.A.U., Hai-ying, B.A.O., Tolgor, B.A.U., Shu-de, Y., Xue, S.U.N., 2012. Anti-tumor activity of tricholoma mongolicum fruit bodies. Food Sci. 21.

Tan, W., Pan, M., Liu, H., Tian, H., Ye, Q., Liu, H., 2017. Ergosterol peroxide inhibits ovarian cancer cell growth through multiple pathways. Onco. Targets. Ther 3467–3474.

Tinoco, G., Warsch, S., Glück, S., Avancha, K., Montero, A.J., 2013. Treating breast cancer in the 21st century: emerging biological therapies. J. Cancer 4, 117.

Wang, X., Bao, H., Bau, T., 2020. Investigation of the possible mechanism of two kinds of sterols extracted from leucocalocybe mongolica in inducing HepG2 cell apoptosis and exerting anti-tumor effects in H22 tumor-bearing mice. Steroids 163, 108692. https://doi.org/10.1016/j.steroids.2020.108692.

Xiong, M., Huang, Y., Liu, Y., Huang, M., Song, G., Ming, Q., Ma, X., Yang, J., Deng, S., Wen, Y., 2018. Antidiabetic activity of ergosterol from pleurotus ostreatus in KK-ay mice with spontaneous type 2 diabetes mellitus. Mol. Nutr. Food Res. 62, 1700444.

Yan, Y., Shi, N., Han, X., Li, G., Wen, B., Gao, J., 2020. UPLC/MS/MS-based metabolomics study of the hepatotoxicity and nephrotoxicity in rats induced by Polygonum multiflorum thunb. ACS Omega 5, 10489–10500.

Yongxia, Z., Jian, X., Suyuan, H., Aixin, N., Lihong, Z., 2020. Isolation and characterization of ergosterol from monascus anka for anti-lipid peroxidation properties. J. Mycol. Med. 30, 101038.

Yuan, Z., Guan, Y., Wang, L., Wei, W., Kane, A.B., Chin, Y.E., 2004. Central role of the threonine residue within the p+ 1 loop of receptor tyrosine kinase in STAT3 constitutive phosphorylation in metastatic cancer cells. Mol. Cell. Biol. 24, 9390–9400.

Zaki, A. H., and Bao, H., 2022. Effect of Isolated and purified Chemical Constituents from The Culinary-Medicinal Mushroom Leucocalocybe mongolica" Fruiting Body on Mammary Epithelial Cells Proliferation (In vitro Study). the 11th International Medicinal Mushroom Conference, in Belgrade, Serbia.

Zhang, Y., Gu, X., Yuan, X., 2007. Phenylalanine activates the mitochondria-mediated apoptosis through the RhoA/Rho-associated kinase pathway in cortical neurons. Eur. J. Neurosci. 25, 1341–1348.
Zhao, Y.-Y., Cheng, X.-L., Vaziri, N.D., Liu, S., Lin, R.-C., 2014. UPLC-based metabonomic applications for discovering biomarkers of diseases in clinical chemistry. Clin. Biochem. 47, 16–26.
Zhao, L., Yuan, X., Wang, J., Feng, Y., Ji, F., Li, Z., Bian, J., 2019. A review on flavones targeting serine/threonine protein kinases for potential anticancer drugs. Bioorg. Med. Chem. 27, 677–685.
Zhu, Y., Li, S., Zhu, C., Wang, W., Zuo, W., Qiu, X., 2020. Metabolomics analysis of the antidepressant prescription danzhi xiaoyao powder in a rat model of chronic unpredictable mild stress (CUMS). J. Ethnopharmacol. 260, 112832.